Crucial Role of the H11-H12 Loop in Stabilizing the Active Conformation of the Human Mineralocorticoid Receptor

Chantal Hellal-Levy, Jérôme Fagart, Anny Souque, Jean-Marie Wurtz, Dino Moras, and Marie-Edith Rafestin-Oblin*

INSERM U478 (C.H.-L., A.S., M.-E.R.-O.)
Faculté de médecine Xavier Bichat
Institut fédératif de recherche 02
B.P. 416, 75780 Paris Cédex 18, France

Institut de Génétique et de Biologie Moléculaire et Cellulaire
(J.F., J.-M.W., D.M.) B.P. 163, 67404 Illkirch Cédex
CU de Strasbourg, France

The crystal structures of ligand-free and agonist-associated ligand-binding domain (LBD) of nuclear receptors (NRs) reveal that the amphipathic helix H12 is folded back toward the LBD core in the agonist-associated conformation, allowing the binding of coactivators. We used alanine scanning mutagenesis to explore the role of the residues of the loop connecting H11 and H12 in the activation of the human mineralocorticoid receptor (hMR), a member of the NRs family. H950A retained the ligand binding and transcriptional activities of the wild-type receptor and interacted with coactivators. In contrast F956A had no receptor functions. Aldosterone bound to the mutant hMRs (L952A, K953A, V954A, E955A, P957A) with nearly the same affinity as to the wild- type receptor and caused a receptor conformational change in these mutant hMRs as it does for the wild-type receptor. But the aldosterone-induced transcriptional activity of the mutant hMRs was lower (L952A, E955A, P957A) than that of the wild-type receptor or completely abolished (K953A, V954A) and their interaction with coactivators was impaired (E955A) or suppressed (L952A, K953A, V954A, P957A). In the light of a hMR-LBD model based on the structure of the progesterone-associated receptor-LBD, we propose that the integrity of the H11-H12 loop is crucial for folding the receptor into a ligand-binding competent state and for establishing the network of contacts that stabilize the active receptor conformation. (Molecular Endocrinology 14: 1210–1221, 2000)

0888-8809/00/$3.00/0
Molecular Endocrinology 14(8): 1210–1221

INTRODUCTION

The human mineralocorticoid receptor (hMR), which mediates the physiological action of aldosterone, belongs to the nuclear receptor (NR) superfamily (1–4). These receptors have a common modular structure with three major functional domains. The most divergent module is the N-terminal A/B region, which contains the constitutive transactivation function AF-1. The central DNA-binding domain (DBD) is highly conserved and composed of two zinc fingers that are involved in DNA binding and receptor dimerization. The ligand-binding domain (LBD) lies in the C-terminal region and takes part in several functions, including nuclear localization, interaction with the heat shock protein 90 (hsp90), homo- and/or hetero-dimerization, and a ligand-dependent activation function AF-2.

The precise mechanisms whereby transcription is stimulated remain unknown. In the absence of hormone, steroid receptors are associated with an inhibitory multiprotein complex composed of hsp90, hsp70, p59, and other factors (5). The binding of the steroid to the hMR induces a change in the receptor conformation that is believed to lead to the dissociation of the multiprotein complex formed with receptor (6, 7). Recent studies have identified two related proteins, a nuclear receptor corepressor (N-CoR) and a silencing mediator for the retinoid and thyroid-hormone receptors (SMRT), that mediate the repression of transcription by thyroid hormone receptor (TR) and retinoic acid receptor (RAR) (8, 9). The nuclear hormone receptors that interact with N-CoR and SMRT now include other members of the NR superfamily, such as COUP-TF, and the thiazolidinedione-peroxisome proliferator-activated receptor γ (PPARγ) (10, 11).

Several crystal structures of NR-LBDs have been described: the ligand-free form (apo receptor) of the retinoid X receptor α (RXRα) and PPARγ, the ligand-bound form (holo receptor) of all-*trans*-retinoic acid receptor γ (RARγ), TRα, ERα, PR, and PPARγ (12–18). All these NR-LBDs have a common fold with 11 to 12 α-helices (numbered H1-H12) and one β-sheet arranged as an antiparallel α-helical "sandwich" in a three-layer structure (19). Ligand binding causes the LBD to adopt a more compact structure; the helix H11 is repositioned in the continuity of H10 and the helix H12, that comprises the autonomous activating domain (AF-2AD), is folded back toward the LBD core. The repositioning of the activation helix H12, together with additional structural changes such as bending of H3, brings it into a distinct receptor environment, thus creating an interface suitable for NR coactivator binding (20). Many coactivators interacting with the nuclear receptors in a ligand-dependent manner have been identified to date. These include steroid receptor-coactivator 1 (SRC-1), transcriptional intermediary factor II (TIF-II)/GRIP-1, and 140-kDa receptor-interacting proteins (RIP-140), TIF1, and CBP/p300 (10, 11).

Because agonist-induced repositioning of the helix 12 is crucial to bring steroid receptors in a suitable conformation for productive interaction with transcriptional machinery, the question arises whether the extended region connecting the helices H11 and H12 (H11-H12 loop), which is highly conserved among steroid receptors, plays a role in the intramolecular process(es) of MR activation. A detailed mutagenesis analysis of the hMR H11-H12 loop was therefore carried out. The ligand-binding properties and transcriptional activities of the mutant hMRs were measured. Their ability to interact with coactivators was assessed as well as their conformational states. In the light of a three-dimensional model of the hMR-LBD, we propose that H11-H12 loop is required to fold the hMR into a ligand-binding competent state and to stabilize the active receptor conformation.

RESULTS

Steroid Binding to Mutant hMRs

The sequence alignment of the H11-H12 loop from MRs of numerous species and also from hGR, hAR, hERα, and hPR is presented in Fig. 1. The residues of the H111-H12 loop are highly conserved among MRs. hGR has one residue and hERα three residues less than the hMR, whereas the H11-H12 loops in hAR and hPR have the same length as in the hMRs. Residues of the hMR H11-H12 loop were replaced by alanine and the corresponding mutant receptors referred to as H950A, L952A, K953A, V954A, E955A, F956A, and P957A. Wild-type and mutant hMRs were expressed *in vitro* and tested for their expression level and ability to bind aldosterone. As observed in Fig. 2A, similar amounts of the wild-type and mutant hMRs were synthesized according to the protein band intensity with a molecular mass of 110 kDa. H950A, L952A and E955A retained the aldosterone binding capacity of the wild-type receptor (Fig. 2B). K953A, V954A, and P957A displayed 50–75% of the aldosterone binding capacity. In contrast F956A was unable to bind aldosterone (Fig. 2B). Moreover, the mutant hMRs transiently expressed in COS-7 cells were tested for their ability to bind aldosterone. L952A, K953A, V954A, and P957A displayed 35–65% of the aldosterone binding capacity. H950A and E955A retained 100% of the aldosterone binding capacity whereas F956A has completely lost this function (data not shown).

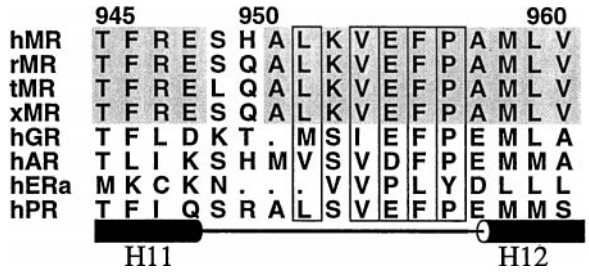

Fig. 1. Sequence Alignment of Amino Acids of the H11-H12 Loop Region of Steroid Receptors

The alignment includes MRs from many organisms plus hGR, hAR, hERα, and hPR. The abbreviations are h, *Homo sapiens*; r, *Rattus norvegicus*; t, *Tupaia belangeri*; x, *Xenopus laevis*. The positions of the ends of the helices H11 and H12 are illustrated *below* the alignment. The *numbering above* the alignment is for hMR. Identical residues in the MR family are in *gray*. Those similar in all sequences are *boxed*. The figure was prepared using ALSCRIPT (54).

The aldosterone-binding properties of the mutant hMRs expressed *in vitro* was further characterized by measuring the dissociation constant at equilibrium (K_d) and the half-life time ($t_{1/2}$) of the hormone-receptor complexes. Aldosterone bound to L952A, K953A, V954A, E955A, and P957A with an affinity 2- to 5-fold lower than that of the wild-type receptor (Table 1). Aldosterone dissociated from L952A, K953A, and P957A much more rapidly ($t_{1/2}$ values of 3–10 min) than from the wild-type receptor (120 min) (Table 1) and the aldosterone-E955A complex was characterized by a half-life time of 42 min.

As the heat shock protein hsp90 plays a crucial role to fold the receptor into a ligand binding-competent state (21), we compared the sedimentation profile of F956A with that of the wild-type receptor. It has been reported that the hsp90-MR complexes sedimented on sucrose gradient in the 8–10S region, whereas upon hsp90 dissociation the receptor sedimented in the 4S region (22). The ligand-free wild type and F956A were synthesized *in vitro* in the presence of ^{35}S methionine and analyzed by sucrose gradient centrifugation. F956A sedimented in the 8–10S region as did the wild-type receptor (Fig. 3), suggesting that replace-

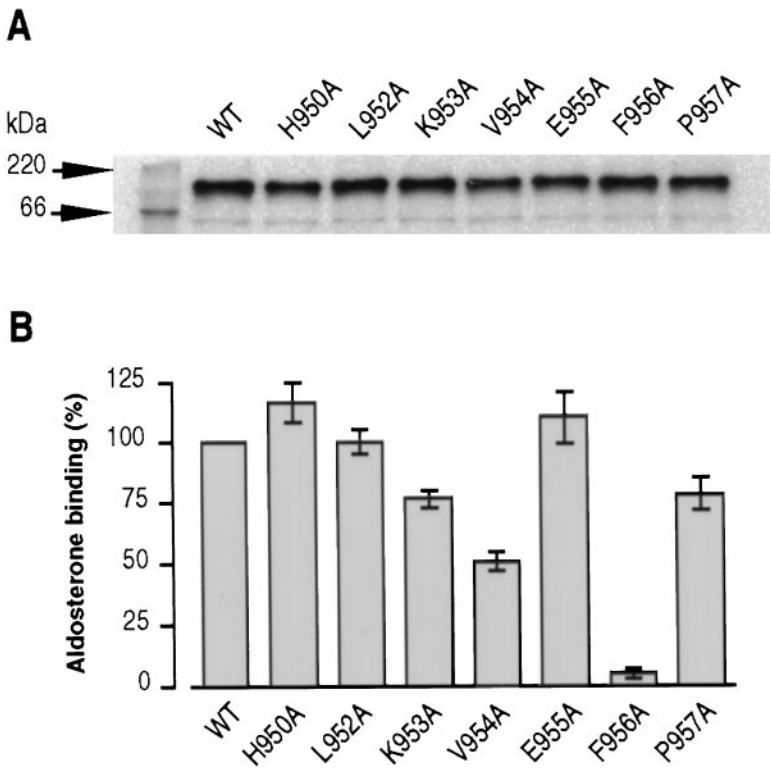

Fig. 2. Binding of Aldosterone to the Wild-Type and Mutant hMRs

A, [^{35}S]-labeled wild-type and mutant hMRs were synthesized *in vitro* and analyzed by electrophoresis in a 12.5% (wt/vol) polyacrylamide gel. The molecular mass markers are indicated on the *left-hand* side of the figure. B, The wild-type and mutant hMRs were synthesized *in vitro*. The lysate was diluted 2-fold with TEGWD buffer and incubated with 10 nM [^{3}H]-aldosterone for 30 min at 20 C. Bound and free steroids were separated by the dextran-charcoal method. Nonspecific binding was measured in a parallel experiment without any receptor expressing vector. Results are given as specific [^{3}H]-aldosterone binding compared with 100% binding to wild-type hMR.

Table 1. Characteristics of Aldosterone Binding to the Wild-Type and the Mutant hMRs

	K_d (nM)	$t_{1/2}$ (min)
WT	0.80 ± 0.03	120
L952A	2.43 ± 0.07	4
K953A	1.45 ± 0.29	10
V954A	0.87 ± 0.44	ND
E955A	1.67 ± 0.44	42
P957A	3.61 ± 0.10	3

The wild-type and the mutant hMRs were expressed in the rabbit reticulocyte lysate. The aldosterone dissociation constant at equilibrium (K_d) was determined after incubation of the *in vitro* expressed receptors with increasing concentrations of [^{3}H]aldosterone for 4 h at 4 C. The half-lives of aldosterone-receptor complexes ($t_{1/2}$) were determined as described in *Materials and Methods*. ND, Not detected.

ment of Phe956 by an alanine does not prevent the hsp90-receptor interaction.

Thus, substitution of the H11-H12 loop residues does not modify the expression level of the mutant hMRs compared with the wild-type receptor. Replacement of Phe956 by alanine induced a complete loss of the receptor ligand-binding capacity that was not due to the inability of this mutant hMR to interact with hsp90. Replacement of His950 and Glu955 by alanine does not alter the ligand-binding capacity of the receptor whereas replacement of Leu952, Lys953, Val954, and Pro957 led to a decrease of this function. Interestingly, an increase of the aldosterone dissociation rate from L952A, K953A, E955A, and P957A was observed, whereas the aldosterone dissociation constant at equilibrium for these mutant hMRs was of the same order of magnitude as that observed for the wild-type receptor.

Conformation Analysis of the Mutant hMRs by Limited Proteolysis Assays

We investigated whether replacement Phe956 by alanine induced a change in the receptor conformation leading to the lack of aldosterone binding. The sensitivity of F956A to chymotrypsin was examined and compared with that of the wild type. The ^{35}S-labeled wild-type hMR and F956A synthesized *in vitro* were incubated in ligand-free conditions with 15 μg/ml chymotrypsin for 5–30 min, and the digestion products were analyzed by SDS-PAGE (Fig. 4). The wild-type receptor and F956A were both syn-

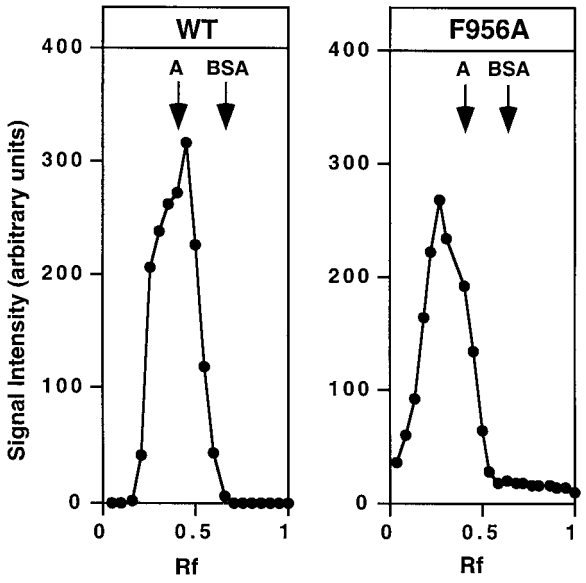

Fig. 3. Sedimentation Gradient Analyses of Mutant hMRs in Ligand-Free Conditions

[^{35}S]-MR, and F956A were synthesized *in vitro* (0.1 ml), were layered onto a 5–20% sucrose gradient equilibrated in TEGWD buffer. Gradients were centrifuged for 1 h, 45 min at 365,000 $\times$ *g* in a VTi 65.2 rotor at 4 C. Collected fractions were analyzed by electrophoresis on a 7.5% (wt/vol) polyacrylamide gel. The band corresponding to the intact or mutant protein was scanned and quantified. The signal intensity was plotted against the relative migration coefficient (Rf). The sedimentation markers were aldolase (A, 7.9S) and BSA (4.6S).

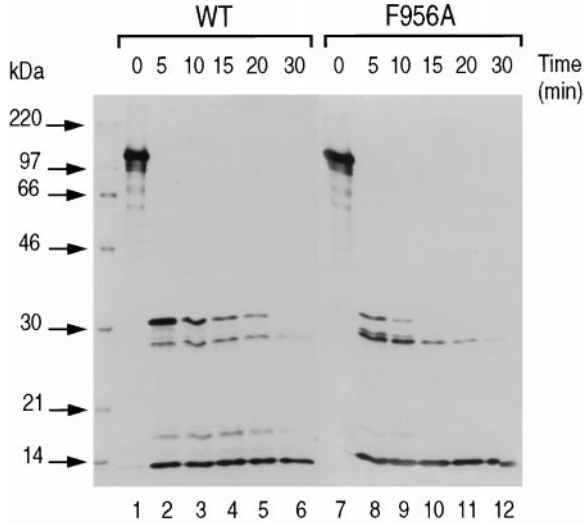

Fig. 4. Chymotrypsin Proteolysis of the Ligand-Free Wild-Type and F956A

[^{35}S]-labeled hMR and F956A were expressed *in vitro* and incubated at 20 C without or with 15 μg/ml chymotrypsin for 5–30 min. The digestion products were analyzed by electrophoresis in a 12.5% (wt/vol) polyacrylamide gel and autoradiographed. The molecular mass markers are indicated on the *left-hand* side of the figure.

thesized at the same level (Fig. 4, lanes 1 and 6). Two major fragments corresponding to molecular masses of 27 and 30 kDa were generated from both the wild-type hMR and F956A, but the abundance of the two fragments differed. After 5 min chymotrypsin treatment, the intensity of the 30-kDa fragment generated from the wild-type receptor was higher than that of the 27-kDa fragment (Fig. 4, lane 2), and the two fragments were completely digested after a 30-min proteolysis (Fig. 4, lane 6). In the case of F956A, the intensity of the 30-kDa fragment was lower than that of the 27-kDa fragment (Fig. 4, lane 8), and the 30- and 27-kDa fragments were completely digested after 15 and 30 min proteolysis, respectively (Fig. 4, lanes 10 and 12). The 30-kDa fragment corresponds to the sequence Ile711-Lys984, which contains the C-terminal part of the hinge region and the entire LBD of the receptor (7). The 27-kDa fragment has not been identified. Proteolysis experiments performed with a truncated hMR, lacking the A/B domain, generated the 30- and 27-kDa fragments, suggesting that the 27-kDa fragment did not encompass the A/B region. Altogether these findings revealed an increase in the receptor sensitivity to proteolysis upon Phe956 substitution, suggesting a change in the receptor compaction.

Binding of aldosterone to the wild-type hMR caused a change in the receptor conformation revealed by an increase in the resistance of the 30-kDa fragment to chymotrypsin (7). As aldosterone bound to L952A, K953A, V954A, and P957A, the ability of aldosterone to modify the conformation of these mutant hMRs was examined. Treatment of ligand-free hMR with 150 μg/ml chymotrypsin for 10 min led to a complete digestion of the receptor (Fig. 5, lanes 2). When the wild-type and mutant hMRs (L952A, K953A, V954A, and P957A) were first incubated with aldosterone and then with chymotrypsin for 10 min treatment, a 30-kDa fragment was detected (Fig. 5, lanes 3–7). The 30-kDa fragment generated from the mutant hMRs was partially (L952A) or completely (K953A, V954A, and P957A) digested after 60 min chymotrypsin treatment, whereas 30-kDa fragment generated from the wild-type receptor was highly resistant (Fig. 5, lanes 8–12). These results suggest that replacement of Leu952, Lys953, Val954, and Pro957 by alanine does not prevent the aldosterone-induced compaction of the receptor. Nevertheless, these aldosterone-mutant hMRs complexes are less resistant to proteolysis than the wild-type receptor associated with aldosterone, suggesting a different or less stable conformation of these mutant receptors compared with the wild-type hMR.

Transcriptional Activation by Mutant hMRs

We examined the activity of the wild-type and mutant hMRs in *cis-trans* cotransfection assays. The mutant

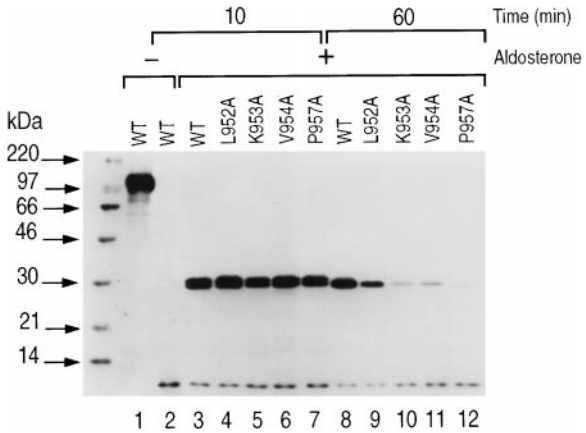

Fig. 5. Chymotrypsin Proteolysis of the Free hMR and Aldosterone-Bound Wild-Type and Mutant hMRs

[^{35}S]-labeled hMR and mutant hMRs L952A, K953A, V954A, and P957A were produced *in vitro* and incubated or not with 10^{-7} M of aldosterone. The resulting complexes were incubated at 20 C without or with 150 μg/ml chymotrypsin for 10 and 60 min. The digestion products were analyzed by electrophoresis in a 12.5% (wt/vol) polyacrylamide gel and autoradiographed. The molecular mass markers are indicated on the *left-hand* side of the figure.

and wild-type cDNA were transiently transfected into COS-7 cells together with a reporter plasmid containing the mouse mammary tumor virus (MMTV) promoter upstream of the luciferase gene. The activity of the mutant hMRs in response to 10^{-6} M aldosterone is reported in Fig. 6A. The aldosterone induced-activity of H950A and E955A was nearly the same as that of the wild-type hMR. L952A and P957A displayed approximately 50% of the wild-type receptor activity; in contrast, K953A, V954A, and F956A have completely lost the receptor activity (Fig. 6A). Dose-response curves were also generated by adding increasing concentrations of aldosterone to transfected cells (Fig. 6B). Aldosterone increased the luciferase activity of the wild-type hMR in a dose-dependent manner with an ED_{50} value of approximately 10^{-10} M. Replacement of His950 by alanine did not modify the aldosterone-induced transactivation activity of hMR, and replacement of Glu955 by alanine induced a shift in the dose-response curve of the aldosterone-induced luciferase activity toward higher concentrations with an ED_{5O} value of approximately 10^{-9} M. The aldosterone-mediated activities of L952A, K953A, V954A, and P957A were low (Fig. 6B). Progesterone, a potent mineralocorticoid antagonist (23), was able to inhibit the aldosterone-induced activity of H950A and E955A by 80%, as it does for the wild-type hMR (data not shown). Thus, except H950A, which retained the transcriptional activity of the wild-type receptor, all the other mutant hMRs, within the H11-H12 loop, displayed a lower transcriptional activity, suggesting that this loop is involved in the hMR activation process.

Interaction of Wild-Type and Mutant hMRs with Coactivators *in Vitro*

Numerous reports have stated that coactivator factors are required for the NRs full activity (10, 11). We therefore examined, by glutathione-*S*-transferase (GST) pull-down assays, whether the wild type and mutant hMRs were able to recruit SRC-1, RIP-140, or TIF1α (24–26). The wild-type hMR did not interact with coactivators in the absence of ligand (Fig. 7A, lanes 3, 6, and 9) or in the presence of progesterone (Fig. 7A, lanes 5, 8, and 11). Incubation of hMR with aldosterone promoted the interaction of the receptor with coactivators (Fig. 7A, lanes 4, 7, and 10). Our results are consistent with those observed with GRIP1 and SCR-1 for the rat MR (27, 28) and other NRs indicating that the receptor-coactivator interaction is agonist dependent (10, 11). As observed for the wild-type hMR, the ligand-free H950A, K953A, and E955A did not interact with hTIF1α (Fig. 7B, lanes 1, 3, and 5). In the presence of aldosterone, H950A interacted with hTIF1α (Fig. 7B, lane 2), and a weak interaction was detected for E955A (Fig. 7B, lane 6). hTIF1α did not interact with aldosterone-associated K953A (Fig. 7B, lane 4), and no interaction of L952A, V954A, and P957A with hTIF1α was detected (data not shown). The interaction profile of the mutant hMRs with RIP140 and SRC-1 was the same as that observed with hTIF1α (data not shown). Altogether, these results showed that, with the exception of H950A and E955A, all the mutant hMRs have lost their ability to bind coactivators.

Three-Dimensional Organization of the H11-H12 Loop

The hMR-LBD homology model, generated using the crystallographic structure of the hPR-LBD as a template, showed the N-terminal part of the loop to be organized as a short helix (from Ser949 to Ala951), with the remainder in an almost extended conformation (Fig. 8). The polar residues face the solvent, whereas the hydrophobic ones are buried and point toward the core of the protein. Phe956 is within the region delimited by the helices H3, H11, and H12 and forms van der Waal contacts with Asn770 (H3), Phe946 (H11), Ser949 and Val954 (H11-H12 loop), Leu960, Val961 and Ile964 (H12), and the aldosterone C21-hydroxyl group (3, 2 Å) (Fig. 9A). Val954 is deeply buried (<10% of solvent accessibility) and is in close contact with Glu763, Leu766, Ser767 and Asn770 (H3), Leu952 and Phe956 (H11-H12 loop) (Fig. 9B). Leu952 is less well buried (24% accessibility) than Val954 and is close to Thr945 (H11) and Val954 (H11-H12 loop) (Fig. 9B). The two charged residues of the H11-H12 loop (Lys953 and Glu955) could form salt bridges with Glu763 and Arg771, respectively, two residues of H3 (Fig. 9B). As in the hPR crystal structure, the backbone oxygen atom of Glu955 forms a strong hydrogen bond with the Asn770 amide group

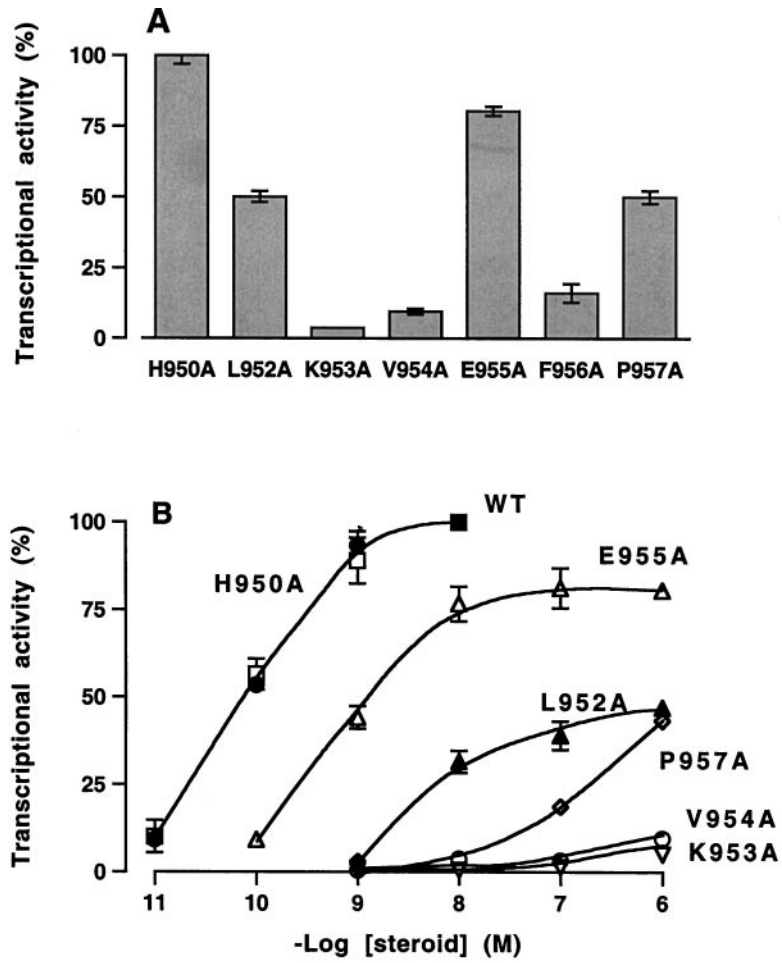

Fig. 6. Transactivation Properties of Wild-Type and Mutant hMRs in Response to Aldosterone

COS-7 cells were transfected with wild-type or mutant hMRs expression vectors, pFC31luc as reporter plasmid, and a β-galactosidase internal reporter to correct for transfection efficiency. A, Before harvesting, cells were treated for 24 h with aldosterone at 10^{-6} M. Transactivation was determined by luciferase activity, normalized to the internal β-galactosidase control, and is expressed as percent of wild-type activity at 10^{-6} M. Each point is the mean ± SEM of three separate experiments. B, Transactivation properties of wild-type and mutant hMRs in response to increasing concentrations of aldosterone were determined by measuring luciferase activity, normalized to the internal β-galactosidase control, and expressed as percent of wild-type activity at 10^{-9} M aldosterone. Each point is the mean ± SEM of three separate experiments.

(Figs. 8 and 9A). From this model, it appeared that there are numerous contacts between the H11-H12 loop residues and also between the residues of this loop and residues of H3, H11, and H12.

DISCUSSION

Studies on the crystal structures and functions of several NRs (20) have revealed that the position of helix H12, which harbors the ligand-dependent activation function, plays a major role in receptor activity. Binding of an agonist to its receptor results in a precise positioning of H12, placing it on the ligand-binding pocket, where it contributes to the area that interacts with coactivators. Our site-directed mutagenesis on the role of the loop connecting the helices H11 and H12 in the activation of the hMR shows that Phe956 is required for hMR to adopt a conformation competent for ligand binding and that numerous residues in this loop are critical for stabilizing the active receptor conformation.

Replacement of Phe956 by alanine within the hMR causes a complete loss of ligand binding and transcriptional activity. The hMR homology model, based on the structural data of the progesterone-associated hPR, revealed that the 21-hydroxyl group of aldosterone is in a favorable position to make van der Waals contacts with Phe956. But it is unlikely that the loss of aldosterone binding capacity upon Phe956 substitution is due solely to the absence of this contact, since progesterone, which lacks the 21-hydroxyl group, is also unable to bind F956A (data not shown). The inability of F956A to bind agonist and antagonist

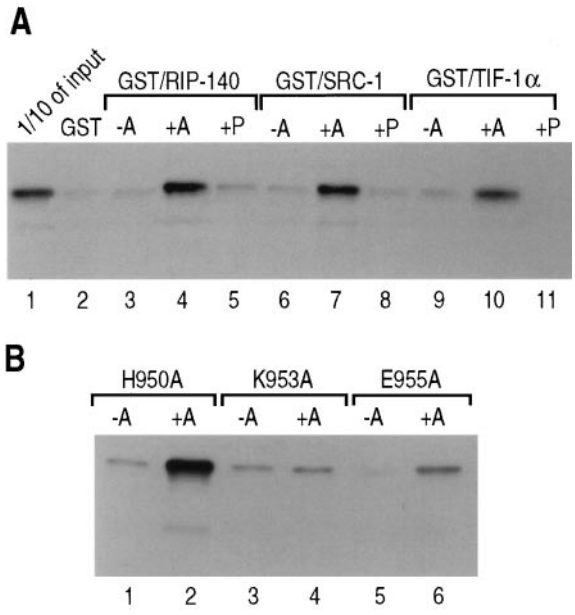

Fig. 7. Interaction of SRC-1, RIP-140, and hTIF1α with Wild-Type and Mutant hMRs

A, GST fusion proteins, which previously had been coupled to Sepharose glutathione beads, were incubated with [^{35}S]methionine-labeled wild-type hMR in the absence (lanes 3, 6, and 9) or presence of 1 μM aldosterone (lanes 4, 7, and 10) or 1 μM progesterone (lanes 5, 8, and 11) for 10 min at 20 C. The glutathione Sepharose beads were washed and boiled in Laemmli buffer. The samples were then analyzed by SDS-PAGE followed by autoradiography. As control, incubation with GST alone (lane 2) and 1/10 of the receptor input used in the assay (lane 1) are shown. B, Interaction of hTIF1α with mutant hMRs (H950A, K953A, and E955A). The interaction assay was performed in the absence of hormone (lanes 1, 3, and 5) and with 1 μM aldosterone (lanes 2, 4, and 6) for 10 min at 20 C. The washed glutathione Sepharose beads were boiled in Laemmli buffer, and samples were analyzed by SDS-PAGE followed by autoradiography. The wild-type and mutant hMRs are expressed at the same level (data not shown).

ligands is not due to a lack of interaction with hsp90 since F956A sedimented at 8–10S as hsp90-receptor complexes (21). The loss of ligand binding capacity upon Phe956 substitution is due to a change in the receptor conformation, as F956A displays a high sensitivity to chymotrypsin compared with the wild-type receptor. Altogether, these results suggest that the residue Phe956 is essential to fold the hMR into a ligand binding competent state.

Replacement of His950 by alanine does not modify the aldosterone binding and transcriptional activities of the wild-type receptor. In contrast, replacement of the other H11-H12 loop residues decreased (Leu952, Glu955, Pro957) or completely abolished (Lys953, Val954) the receptor activity without notably modifying the affinity of the receptor for aldosterone. The different sensitivities of ligand binding and transcriptional activities to substitution of an H11-H12 loop residue have been reported for other steroid receptors. A naturally occurring mutant androgen receptor, in which Val889 (V954 in hMR) is replaced by a methionine, is nearly completely insensitive to androgens, whereas it has a normal binding affinity for androgens (29). Similarly, a mutant GR, in which Ile747 (Val954 in hMR) is replaced by threonine, can bind dexamethasone like the wild-type receptor, but high dexamethasone concentrations are needed to stimulate the transactivation function (30).

The first step after aldosterone binding to the receptor is a change in the receptor conformation, revealed by an increase in the resistance of the receptor to proteolysis (7). The binding of aldosterone to L952A, K953A, V954A, and P957A increases the resistance of the receptor to chymotrypsin, suggesting that aldosterone bound to these mutant hMRs causes a change in receptor compaction in a way similar to the effect of aldosterone bound to the wild-type receptor. But, as aldosterone dissociates more rapidly from mutant hMRs than from the wild-type receptor, it is less effective in protecting these mutant hMRs against proteolysis than the wild-type receptor. Thus, the ability of aldosterone to protect mutant hMRs against proteolysis depends upon the stability of the aldosterone-receptor complex.

There have been several reports that coactivators interact with NRs when receptors are transcriptionally active (31–34). The introduction of a mutation into the TRβ-H12 (35), the vitamin D receptor-H12 (36), and the ER-H3 (37) causes an alteration in the NR activity together with an impaired interaction with coactivators. The loss of these two functions upon mutation of residues within the helices H12 or H3 is not surprising, given the model proposed from structural data that compares the ligand-induced receptor transconformation to a mouse trap mechanism, by which structural changes such as bending of helix H3, bring the helix H12 into a distinct receptor environment creating the areas for coactivator binding. Furthermore, analysis of the structure of agonist-associated PPAR and hERα LBD complexed with a peptide encompassing the coactivator LXXLL region shows that this peptide is bound, in a α-helical conformation, by a hydrophobic groove formed by residues from helices H3, H4, H5, and H12 (38, 39). The present study shows that aldosterone-associated-hMR interacts with SRC-1 RIP140 and hTIF1α. In contrast, neither ligand-free nor antagonist-associated-hMR bind these coactivators, indicating that the hMR-coactivator interaction is agonist dependent. Those mutant hMRs that retain the full transcriptional activity interact with coactivators, as it is observed for H950A. The poor ability of E955A to recruit coactivators is consistent with the lower sensitivity of this mutant hMR (ED_{50} 10^{-9} M) compared with that of the wild- type receptor (10^{-10} M). The inability of L952A, K953A, V954A, and P957A to recruit coactivators, whereas L952A and P957A display 50% of the wild-type receptor activity, might be due to the rapid dissociation of aldosterone from these mutant hMRs and/or to poor receptor-coactivator contacts

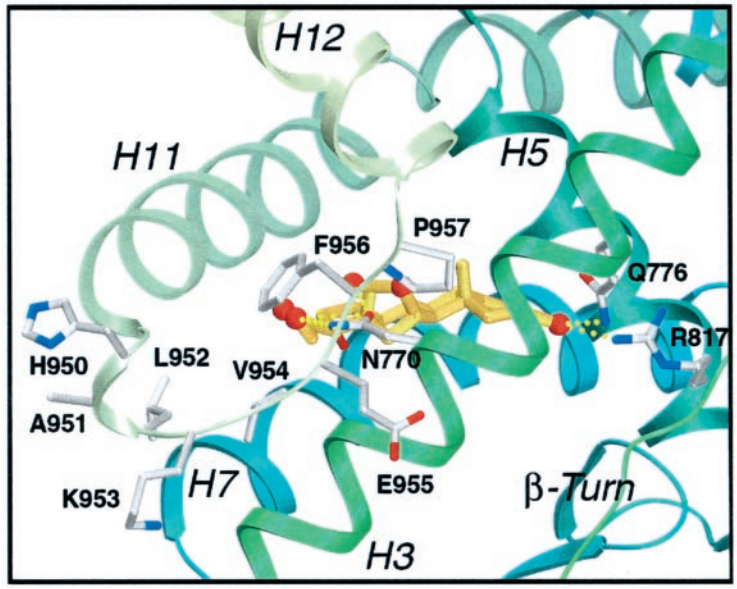

Fig. 8. Aldosterone Docking in the hMR Ligand-Binding Pocket

Diagram showing the overall fold of the hMR-LBD surrounding aldosterone with the α-helices drawn as *ribbons* and the β-strands as *arrows*. Only the residues of the H11-H12 loop and those making hydrogen bonds with aldosterone are shown. The figure was produced with SETOR (52).

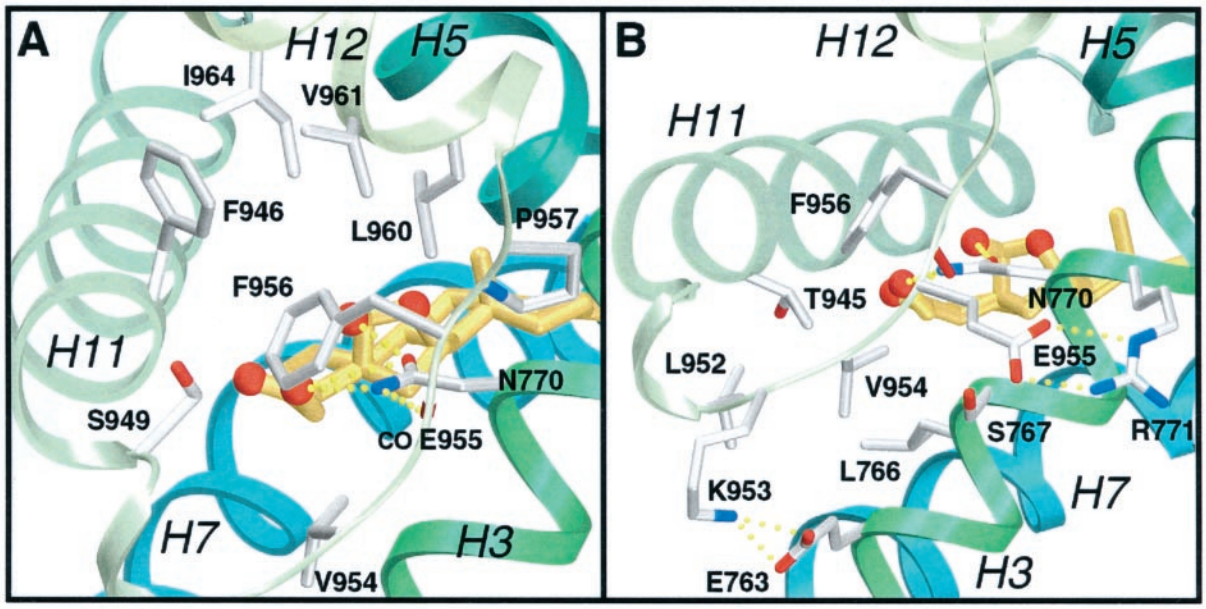

Fig. 9. Organization of the hMR H11-H12 Loop Residues

A, Close-up view of the Phe956 van der Waals contacts and the hydrogen bond network of Asn770. B, Close-up view of the Leu952 and Val954 van der Waals contacts and of the salt bridges. The figures were produced with SETOR (55).

resulting from a modification of the aldosterone-associated-hMR conformation.

The homology model of the hMR LBD reveals numerous contacts in the H11-H12 region that might help to stabilize the aldosterone associated-hMR conformation. There are van der Waals contacts between the hydrophobic residues of the H11-H12 loop (Val 954 with Leu952 and Phe956) and also between residues of the loop and the nearby amino acids of H3, H11, and H12. In addition, the two polar residues of the loop (Lys953 and Glu955) are in suitable positions to make salt bridges with two residues of H3 (Glu763 and Arg771). These contacts may help anchor the H11-H12 loop to helix H3, as mutation of these resi-

dues reduces (Glu955) or abolishes (Lys953) receptor activity without preventing the ligand binding and resistance to proteolysis. Furthermore, the oxygen atom of the Glu955 main chain forms a strong hydrogen bond with Asn770 in helix 3, a residue that is critical in the binding of C21-hydroxylated agonists such as aldosterone (40). This network of contacts is essential for the transition from the ligand-free inactive to the liganded active receptor state. The structure of the ligand-free hMR is unknown: it could be similar to that of the ligand-free RXRα (12), in which helix H11 obstructs the ligand binding cavity, and the H11-H12 loop and H12 point away from the LBD core. The residues of the H11-H12 loop might be compared with a zip fastener, in which each residue of the H11-H12 loop is a link, which helps to promote the precise positioning of H12. It is likely that the accommodation of the receptor around aldosterone is a rate limiting step, as proposed by Ribeiro *et al.* (41) for TRβ, which depends greatly upon the integrity of the H11-H12 loop residues.

The results described here point out the role of the H11-H12 loop in stabilizing the inactive ligand-free and active aldosterone-associated hMR conformation states. With the help of other factors, such as hsp90, the loop H11-H12 maintains the receptor in an open state able to bind agonist and antagonist ligands. It is also essential for establishing the network of contacts required for ordering the activation helix H12 allowing coactivators recruitment. The similarity of the overall organization of NRs and the existence of mutations in other NRs with similar effects on the receptor activation led us to propose that the H11-H12 loop is involved in producing the active state in the other nuclear receptors.

MATERIALS AND METHODS

Chemicals

[1,2-^{3}H]aldosterone (40–60 Ci/mmol), [^{35}S]methionine (1,000 Ci/mmol) and [^{14}C]-labeled low range protein molecular mass markers were purchased from Amersham Pharmacia Biotech (Les Ulis, France). Nonradioactive aldosterone, progesterone, trypsin, and chymotrypsin were obtained from Sigma (St. Louis, MO. Entensify Universal Autoradiography Enhancer was obtained from Du Pont-New England Nuclear (Boston, MA). Purified oligonucleotides and products for cell culture were from Life Technologies, Inc. (Cergy Pontoise, France). The protection mammalian transfection system, the TNT T7-coupled rabbit reticulocyte lysate system and isopropyl β-D-thiogalactoside were purchased from Promega Corp. (Charbonnières, France). To avoid steroid adsorption, steroid solutions prepared in ethanol were dried and the steroids were suspended in 50% (vol/vol) polyethylene glycol 300 prepared in TEG buffer (20 mM Tris-HCl, 1 mM EDTA, and 10% glycerol, pH 7.4) to give a final concentration of 5% in the lysate.

Expression and Reporter Constructs

The plasmid pchMR was constructed by excising a 3.6-kb *Hin*dIII-*Hin*dIII fragment containing the entire coding sequence of the hMR gene and about 270 bp and 400 bp of the 5′- and 3′-untranslated regions from plasmid 3750 (1). This fragment was subcloned into the expression vector pcDNA3 (Invitrogen, NV leek, The Netherlands). pFC31Luc, which contains the MMTV promoter driving the luciferase gene, was obtained from H. Richard-Foy (LMBE, Toulouse, France) (42).

Site-Directed Mutagenesis

Site-specific mutagenesis of the hMR was performed by the method of Nelson and Long (43). The mutant hMR fragments were obtained by PCR amplification using GeneAmp (Perkin-Elmer Cetus, Norwalk, CT). Four primers were used: a reverse hybrid primer downstream of an *Afl*II enzyme restriction site, composed of a nucleotide sequence complementary to the cDNA reverse strand and a single 5′-20 nucleotide sequence: (5′-GGGGTACTAGTAACCCGGGCACCTCTGCCA GCTCTGCCC-3′), a forward primer upstream of a BpU1102I enzyme restriction site: (5′-ACGAAGTGTTTCTACTGGATC-3′), a reverse primer of identical sequence to the single sequence 5′-20 nucleotide: (5′-GGGGTACTAGTAACCCGGGC-3′), and a forward mutagenic primer with base mismatch was used as follows:

H950A:5′-ACCTTCCGAGAGTCCGCTGCGCTGAAG GTA-3′,
L952A: 5′-TCCCATGCGGCGAAGGTAGAGTTCCCC-3′,
K953A: 5′-TCCCATgCgCTGgCggTAgAgTTCCC C-3′,
V954A: 5′-TCCCATgCgCTgAAggCAgAgTTCCCC-3′,
E955A: 5′-CTgAAGGTAGCGTTCCCCGCAATGCTG-3′,
F956A: 5′-CTGAAGGTAGAGGCCCCCGCAATGCTG-3′
P957A: 5′-CTgAAggTAgAgTTCgCCgCAATgCTg-3′).

The amplified products were digested with *BpU1102* and *Afl*II, purified by agarose gel electrophoresis, subcloned into the *BpU1102* and *Afl*II sites pchMR vector and transformed into electrocompetent JM109 cells. The presence of the specific mutation and the lack of random mutations were checked by DNA sequence analysis (Genome Express, Grenoble, France).

Cell Culture and Transfection

COS-7 cells were cultured in DMEM (Life Technologies, Inc., Cergy Pontoise, France) supplemented with 10% heat-inactivated FCS, 2 mM glutamine, 100 IU/ml penicillin, and 100 μg/ml streptomycin in a humidified atmosphere with 5% CO_2. Cells were maintained in the medium supplemented with 10% charcoal-stripped FCS 4 h before and thoughout the transfection procedure. Cells were transfected by the phosphate calcium precipitation method (Promega Corp. system). The phosphate solution, prepared for six-well trays, contained 5 μg of one of the receptor expression vectors (wild-type or mutant pchMR), 10 μg pFC31Luc (42) that contained the MMTV promoter driving the luciferase gene, and 5 μg pSVβ, including the gene coding for β-galactosidase. The steroids to be tested were added to the cells 12 h after transfection and incubation continued for 24 h. Cell extracts were then prepared and assayed for luciferase (44) and β-galactosidase activities (45). To standardize for transfection efficiency, the relative light units, obtained in the luciferase assay, were divided by the optical density obtained in the β-galactosidase assay.

Coupled Cell-Free Transcription and Translation

Plasmids (1 μg) containing cDNA coding for the full-length hMR (1) or mutant hMRs were transcribed using T7 RNA polymerase, and the mRNA was simultaneously translated in rabbit reticulocyte lysate for 1 h at 30 C according to the manufacturer's instructions. The reactions were conducted with unlabeled or [^{35}S]-labeled methionine in the translation mixture, depending on the experiment. The protein concentration of the rabbit reticulocyte lysate, determined by the

Bradford method (46) with BSA as standard, was about 50–70 mg/ml.

In Vitro Hormone-Binding Assay

Reticulocyte lysates containing the wild-type or mutant hMRs were diluted 2-fold with TEGWD buffer (20 mM sodium tungstate and 1 mM dithiothreitol in TEG) and incubated for 30 min at 20 C with 10 nM [^{3}H]aldosterone. Nonspecific binding was measured in a parallel experiment with a transcription and translation in the reticulocyte lysate without receptor. Bound and free steroids were separated by the dextran-charcoal method: 25 μl lysate were stirred for 5 min with 50 μl 4% Norit A, 0.4% Dextran-T70 in TEG buffer, and centrifuged at 4,500 $\times$ *g* for 5 min at 4 C. Bound steroid was measured by counting the radioactivity of the supernatant. Radioactivity was measured, in disintegrations per min, in a liquid scintillation spectrometer (LKB, Rockville, MD) after adding 5 ml OptiPhase HiSafe (counting efficiency $\sim$ 50%).

Hormone Binding in Whole Cells

COS-7 cells transiently transfected as described above were incubated for 30 min at 20 C with 10 nM [^{3}H]aldosterone. The cells were rinsed twice with 1 ml ice-cold PBS (pH 7.4), and bound steroids were extracted by incubating the cells with 0.5 ml ethanol at 20 C for 30 min. The radioactivity of the ethanol extracts was measured in a LKB liquid scintillation spectrometer after adding 5 ml OptiPhase HiSafe (counting efficiency $\sim$ 50%).

Steroid-Binding Characteristics at Equilibrium

Reticulocyte lysates containing the wild-type or mutant hMRs were diluted 2-fold with ice-cold TEGWD buffer and incubated for 4 h at 4 C with [^{3}H]aldosterone (0.1–100 nM). Bound (B) and unbound (U) steroids were separated by the dextran-charcoal method. The change in B as a function of U was analyzed (47) and the dissociation constant at equilibrium (K_d) calculated.

Kinetic Experiments

Reticulocyte lysates containing the wild-type or mutant hMRs were diluted 2-fold with ice-cold TEGWD buffer and incubated with 10 nM [^{3}H]aldosterone for 1 h at 20 C. The lysate was then divided in two. One half was kept at 20 C to measure the stability of the [^{3}H]aldosterone-MR complexes, and the other was incubated with 10 μM aldosterone for various times. After each incubation period, bound and free steroid were separated by the charcoal dextran method. Parallel incubations containing [^{3}H]aldosterone plus a 1000-fold excess of unlabeled aldosterone were used to calculate the nonspecific binding. The half-lives of the steroid-receptor complexes ($t_{1/2}$) were calculated from the equation $B(t)\hat{E} = \hat{E}B(0)\, e^{-(k-1t)}$, where B(0) and B(t) represent the specific steroid binding at times 0 and t of the dissociation period. B(t) is corrected for the stability of steroid binding at each dissociation time.

Sucrose Gradient Centrifugation

Samples were layered onto a 5–20% sucrose gradient prepared in TEGW buffer, and the gradients were centrifuged in a VTi 65.2 rotor at 4 C for 1 h, 45 min at 365,000 $\times$ *g*. Three-drop fractions were collected by piercing the bottom of each tube. Each collected fraction was analyzed by electrophoresis. Aldolase (A, 7.9S) and BSA (4.6S) were used as external sedimentation markers.

Limited Proteolytic Digestion of Translated hMR

[^{35}S]-labeled wild-type or mutant hMRs synthesized *in vitro* were incubated with or without unlabeled aldosterone (10^{-7} M) for 10 min at 20 C. Chymotrypsin (20 μg/ml or 150 μg/ml) was added to 9 μl [^{35}S]-labeled translation mix incubated with or without aldosterone for various times at 20 C. Aliquots of the digestion product (1 μl) were removed and mixed with 20 μl protein loading buffer, boiled for 5 min, immediately loaded onto a 12.5% SDS-polyacrylamide gel, and subjected to electrophoresis. The gels were then fixed for 30 min in methanol/acetic acid/distilled water (30:10:60), treated with Entensify Universal Autoradiography Enhancer, dried, and autoradiographed at $-$80 C overnight.

Production of GST Fusion Proteins

The vectors pGEX2TK containing GST, GST fused with the RIP-140 amino acid sequence 683-1158 (GST-RIP-140), and GST fused with the hTIF1α amino acid sequence 630–854 (GST-hTIF1α) were provided by V. Cavaillès (48). GST-SRC-1 encoding a fusion protein containing GST and residues 570–780 of hSRC-1 was provided by M. G. Parker (49). GST and GST fusion proteins were expressed as described by Kaelin *et al.* (50). Overnight cultures of *Escherichia coli* expressing the recombinant GST plasmids were diluted in Luria-Bertani medium (LB). Cultures at an absorbance at 600 nm of 0.8–1.2 were induced for 3 h with isopropyl β-D-thiogalactoside (0.1 mM final concentration). Bacteria were then collected by centrifugation, suspended 1:10 in NETN (0.5% Nonidet P-40 (NP40), 1 mM EDTA, 20 mM Tris-HCl, 100 mM NaCl, pH 8.0) containing protease inhibitors. The suspension was sonicated and then centrifuged. Protein concentration was estimated by the Bradford method, and the bacterial proteins were separated by SDS-PAGE and visualized by Coomassie blue staining.

GST Pull-Down Assays

An aliquot of crude bacterial extract (1 ml) containing GST fusion proteins was incubated for 30 min at 4 C with 100 μl glutathione-Sepharose beads, previously washed three times, in NETN [final concentration 1:1 (vol/vol)]. The glutathione-Sepharose beads were then washed three times with NETN. The wild-type and mutant hMRs were transcribed, translated, and ^{35}S-labeled in rabbit reticulocyte lysate following the manufacturer's instructions. The resulting receptors were incubated without (ethanol: no hormone) or with 1 μM aldosterone or progesterone for 10 min at 20 C and then with the fusion proteins on glutathione-Sepharose beads for 1 h at 4 C. The beads were washed, suspended in 20 μl loading buffer, boiled for 3 min, and analyzed by SDS-PAGE. Signals were amplified with Entensify, and gels were autoradiographed at $-$80 C overnight.

hMR Homology Model

The hMR-LBD homology model and the docking of the ligands were prepared as previously described (40). Briefly, the hMR-LBD homology model was generated by the Modeller package (version 4.0) (51) using the hPR crystal structure as a template (G. Auzou, J. Fagart, A. Souque, C. Hellal-Levy, J. M. Wurtz, D. Moras, and M. E. Rafestin-Oblin, manuscript in preparation). Aldosterone was docked manually in the pocket using the probe-accessible and van der Waals vol-

umes as guides; these volumes were generated with VOIDOO (52). The side chains in the vicinity of the ligand were positioned in favorable orientation using a rotamer library of the O package (53). The Charmm package (QUANTA/CHARMM package, Molecular Simulation, Inc., Burlington, MA) was used for all calculations. The complex was energy minimized in 2000 steps with a dielectric constant of 2, using the Powell procedure. During the minimization process, the hydrogen bonds were defined by upper harmonic distance restraints (60 kcal $Å^{-2}$ force constant), and the overall structure of the LBD was maintained by harmonic position restraints (30 kcal $Å^{-2}$ force constant) of the Cα atoms of residues defining the secondary structure elements.

Acknowledgments

We are grateful to M. G. Parker, V. Cavailles, H. Richard Foy, and F. Gouilleux for providing plasmids. We would like to thank A. T. Beggah for technical advice on the mutagenesis experiments and M. G. Catelli for stimulating discussions and critically reading the manuscript. We also thank O. Parkes for editorial assistance.

Received January 12, 2000. Revision received April 13, 2000. Accepted April 27, 2000.

Address requests for reprints to: Corresponding author: M. E. Rafestin-Oblin; INSERM U478, Faculté de médecine Xavier Bichat, B. P. 416, 16 rue Henri Huchard, 75870 Paris Cédex 18, France. E-mail: oblin@bichat.inserm.fr.

This work was suported by INSERM (APEX 98–34, MERO) and by the Fondation pour la recherche medicale (C.H.L.).

REFERENCES

1. Evans RM 1988 The steroid and thyroid hormone receptor superfamily. Science 240:889–895
2. Tsai MJ, O'Malley BW 1994 Molecular mechanism of action of steroid/thyroid receptor superfamily. Annu Rev Biochem 63:451–486
3. Mangelsdorf DJ, Thummel C, Beato M, Herrlich P, Schutz G, Umesono 3 K, Blumberg B, Kastner P, Mark M, Chambon P, Evans RM 1995 The nuclear receptor superfamily: the second decade. Cell 83:835–839
4. Ribeiro RCJ, Kushner PJ, Baxter JD 1995 The nuclear hormone receptor gene superfamily. Annu Rev Med 46: 443–453
5. Pratt WB, Toft DO 1997 Steroid receptor interactions with heat shock protein and immunophilin chaperones. Endocr Rev 18:306–360
6. Trapp T, Holsboer F 1995 Ligand-induced conformational changes in the mineralocorticoid receptor analyzed by protease mapping. Biochem Biophys Res Commun 215:286–29
7. Couette B, Fagart J, Jalaguier S, Lombès M, Souque A, Rafestin-Oblin ME 1996 Ligand-induced conformational change in the human mineralocorticoid receptor occurs within its hetero-oligomeric structure. Biochem J 315: 421–427
8. Horlein AJ, Naar AM, Heinzel T, Torchia J, Gloss B, Kurokawa R, Ryan A, Kamei Y, Soderstrom M, Glass CK, Rosenfeld MG 1995 Ligand-independent repression by the thyroid hormone receptor mediated by a nuclear receptor co-repressor. Nature 377:397–404
9. Chen JD, Evans RM 1995 A transcriptional co-repressor that interacts with nuclear hormone receptors. Nature 377:454–457
10. Schibata H, Spencer TE, Onate SA, Jenster G Tsai Sy, Tsai Mj, O'malley BW 1997 Role of co-activators and co-repressors in the mechanism of steroid/thyroid receptor action. Recent Prog Horm Res 52:141–165
11. Torchia J, Glass C, Rosenfeld MG 1998 Co-activators and co-repressors in the integration of transcriptional response. Curr Opin Cell Biol 10:373–383
12. Bourguet W, Ruff M, Chambon P, Gronmeyer H, Moras, D 1995 Crystal structure of the ligand-binding domain of the human nuclear receptor RXR-α. Nature 375:377–382
13. Renaud JP, Rochel N, Ruff M, Vivat V, Chambon P, Gronemeyer H, Moras D 1995 Crystal structure of the RAR-gamma ligand-binding domain bound to all-trans retinoic acid. Nature 378:681–689
14. Wagner RL, Apriletti JW, McGrath ME, West BL, Baxter JD, Fletterick RJ 1995 A structural role for hormone in the thyroid hormone receptor. Nature: 378:690–697
15. Brzozowski AM, Pike ACW, Dauter Z, Hubbard RE, Bonn T, Engstrom O, Ohman L, Greene GL, Gustafsson JA, Carlquist M 1997 Molecular basis of agonism and antagonism in the oestrogen receptor. Nature 389:753–758
16. Williams SP, Sigler PB 1998 Atomic structure of progesterone complexed with its receptor. Nature 393:392–396
17. Tanenbaum DM, Wang Y, Williams SP, Sigler PB 1998 Crystallographic comparison of the estrogen and progesterone receptor's ligand binding domains. Proc Natl Acad Sci USA 95:5998–6003
18. Nolte RT, Wisely GB, Westin S, Cobb JE, Lambert MH, Kurokaw AR, Rosenfeld MG, Willson TM, Glass CK, Milburn MV 1998 Ligand binding and co-activator assembly of the peroxisome proliferator-activated receptor-γ. Nature 395:137–143
19. Wurtz JM, Bourguet W, Renaud JP, Vivat V, Chambon P, Moras D, Gronemeyer H 1996 A canonical structure for the ligand-binding domain of nuclear receptors. Nat Struct Biol 3:87–94
20. Moras D, Gronemeyer H 1998 The nuclear receptor ligand -binding domain: structure and function. Curr Opin Cell Biol 10:384–391
21. Couette B, Jalaguier S, Hellal-Levy C, Lupo B, Fagart J, Auzou G, Rafestin-Oblin ME 1998 Folding requirements of the ligand-binding domain of the human mineralocorticoid receptor. Mol Endocrinol 12:855–863
22. Rafestin-Oblin ME, Couette B, Radanyi C, Lombès M, Baulieu EE 1989 Mineralocorticoid receptor of the chick intestine. Oligomeric structure and transformation. J Biol Chem 264:9304–9309
23. Souque A, Fagart J, Coette B, Davioud E, Sobrio F, Marquet A, Rafestin-Oblin ME 1995 The mineralocorticoid activity of progesterone derivates depends on the nature of the C18 substituent. Endocrinology 136: 5651–5658
24. Onate A, Tsai SY, Tsai MJ, O'Malley BW 1995 Sequence and characterization of a coactivator for the steroid hormone receptor suparfamily. Science 270:1354–1357
25. Cavailles V, Dauvois S, Danielan PS, Parker MG 1994 Interaction of proteins with transcriptionally active estrogen receptors. Proc Natl Acad Sci USA 91:10009–10013
26. Thenot S, Henriquet C, Rochefort H, Cavailles V 1997 Differential interaction of nuclear receptors with putative human transcriptional coactivator hTIF1. J Biol Chem 272:12062–12068
27. Hong H, Kohli K, Garabedian MJ, Stallcup MR 1997 GRIP1, a transcriptional coactivator for the AF-2 transactivation domain of steroid, thyroid, retinoid, and vitamin D receptors. Mol Cell Biol 17:2735–2744
28. Ding XF, Anderson CM, Ma H, Hong H, Uht RM, Kushner PJ, Stallcup MR 1998 Nuclear receptor-binding sites of coactivators glucocorticoid receptor interacting protein 1 (GRIP1) and steroid receptor coactivator 1 (SRC-1): multiple motifs with different binding specificities. Mol Endocrinol 12:302–313
29. Zhou ZX, Lane MV, Kemppainen JA, French FS Wilson EM 1995 Specificity of ligand-dependent androgen receptor stabilization:receptor domain interactions influ-

ence ligand dissociation and receptor stability. Mol Endocrinol 9:208–218
30. Roux S, Terouanne B, Couette B, Rafestin-Oblin ME Nicolas JC 1999 Conformational change in the human glucocorticoid receptor induced by ligand binding is altered by mutation of isoleucine 747 by a threonine. J Biol Chem 274:10059–10065
31. Le Douarin B, Zechel C, Garnier JM, Lutz Y, Tora L, Pierrat P, Heery D, Gronemeyer H, Chambon P, Losson R 1995 The N-terminal part of TIF1, a putative mediator of the ligand-dependent activation function (AF-2) of nuclear receptors, is fused to B-raf in the oncogenic protein T18. EMBO J 14:2020–2033
32. Cavaillès V, Dauvois S, L'Horset F, Lopez G, Hoare S, Kushner PJ, Parker MG 1995 Nuclear factor RIP140 modulates transcriptional activation by the estrogen receptor. EMBO J 14:3741–3751
33. Voegel JJ, heine MJ, Zechel C, Chambon P, Gronemeyer H 1996 TIF2, a 160 kDa transcriptional mediator for the ligand-dependent activation function AF-2 of nuclear receptors. EMBO J 14:3667–3675
34. Joyeux A, Cavaillès V, Balaguer P, Nicolas JC 1997 RIP140 enhances nuclear receptor-dependent transcription *in vivo* in yeast. Mol Endocrinol 11:193–220
35. Collingwood TN, Rajanayagam O, Adams M, Wagner R, Cavaillès V, Kalkhoven E, Matthews C, Nystrom E, Stenlof K, Lindstedt G, Tisell L, Fletterick RJ, Parker MG 1997 A natural transactivation mutation in the thyroid hormone β receptor: impaired interaction with putative transcriptional mediators. Proc Natl Acad Sci USA 94:248–253
36. Masuyama H, Brownfield M, St-Arnaud R, MacDonald PN 1997 Evidence for ligand-dependent intramolecular folding of the AF-2 domain in vitamin D receptor-activated transcription and coactivator interaction. Mol Endocrinol 11:1507–1517
37. Henttu PMA, Kalkhoven E, Parker MG 1997 AF-2 activity and recruitement of steroid receptor coactivator 1 to the estrogen receptor depend on a lysine residue conserved in nuclear receptors. Mol Cell Biol 1832–1839
38. Nolte RT, Wisely GB, Westin S, Cobb JE, Lambert MH, Kurokawa R, Rosenfeld MG, Willson TM, Glass CK, Milburn MV 1998 Ligand binding and coactivateur assembly of the peroxisome proliferator-activated receptor-γ. Nature 395:137–143
39. Shiau AK, Barstad D, Loria PM, Cheng L, Kushner PJ, Agard DA, Greene GL 1998 The structural basis of estrogen receptor/coactivator recognition and the antagonism of this interaction by tamoxifen. Cell 95:927–937
40. Fagart J, Wurtz JM, Souque A, Hellal-Levy C, Moras D, Rafestin-Oblin ME 1999 Antagonism in the human mineralocorticoid receptor. EMBO J 17:3317–3325
41. Ribeiro RCJ, Apriletti JW, Wagner RL, Feng W, Kushner PJ, Nilsson S, Scanlan TS, West BL, Fletterick RJ, Baxter JD 1998 X-ray crystallographic and functional studies of thyroid hormone receptor. J Steroid Biochem Mol Biol 65:133–141
42. Gouilleux F, Sola B, Couette B Richard-Foy H 1991 Cooperation between structural elements in hormono-regulated transcription from the mouse mammary tumor virus promoter. Nucleic Acids Res 19:1563–1569
43. Nelson RM, Long GL 1989 A general method of site-specific mutagenesis using a modification of the thermus aquaticus polymerase chain reaction. Anal Biochem 180: 147–151
44. De Wet JR, Wood KV, Deluca M, Helsinki DR Subramani S 1987 Firefly luciferase gene: structure and expression in mammalian cells. Mol Cell Biol 7:725–737
45. Herbomel P, Bourachot B Yanif M 1984 Two distinct enhancers with different cell specificities coexist in the regulatory region of polyoma. Cell 39:653–662
46. Bradford MM 1976 A rapid and sensitive method for the quantitation of microgram quantities of protein utilizing the principle of protein-dye binding. Anal Biochem 72: 248–254
47. Claire M, Rafestin-Oblin ME, Michaud A, Corvol P, Venot A, Roth-Meyer C, Boisvieux JF Mallet A 1978 Statistical test of models and computerized parameter estimation for aldosterone binding in rat kidney. FEBS Lett 88: 295–299
48. Thénot S, Henriquet C, Rochefort H, Cavaillès V 1997 Differential interaction of nuclear receptors with the putative transcriptional coactivator hTIF1. J Biol Chem 272: 12062–12068
49. Kalkhoven E, Valentine JE, Heery DM, Parker MG 1998 Isoforms of steroid receptor co-activator 1 differ in their ability to potentiate transcription by the oestrogen receptor. EMBO J 17:232–243
50. Kaelin WG, Pallas DC, DeCaprio JA, Kaye FJ, Livingston DM 1991 Identification of cellular proteins that can interact specifically with the T/E1A-binding region of the retinoblasma gene product. Cell 64:521–532
51. Sali A, Blundell TL 1993 Comparative protein modelling by satisfaction of spatial restraints. J Mol Biol 234: 779–815
52. Kleywegt, GJ, Jones TA 1994 Detection, delineation, measurement and display of cavities in macromolecular structures. Acta Crystallogr D50:178–185
53. Jones TA, Zou JY, Cowan SW, Kjeldgaard M 1991 Improved methods for binding protein models in electron density maps and the location of errors in these models. Acta Crystallogr A7:110–119
54. Barton GJ 1993 ALSCRIPT: a tool to format multiple sequence alignments. Protein Eng 6:37–40
55. Evans SV 1993 SETOR: hardware lighted three-dimensional solid model representations of macromolecules. J Mol Graphics 11:134–138